

## 胶体量子点垂直腔面发射激光器的设计与仿真

项国洪<sup>1,2,3</sup>, 贾思琪<sup>1,2</sup>, 李德鹏<sup>1,2</sup>, 马精瑞<sup>1,2</sup>, 刘湃<sup>1,2</sup>, 王恺<sup>1,2</sup>, 郭海成<sup>3</sup>, 余明斌<sup>4,5</sup>, 孙小卫<sup>1,2\*</sup><sup>1</sup>南方科技大学能源转换与存储技术教育部重点实验室, 广东 深圳 518055;<sup>2</sup>南方科技大学电子与电气工程系广东省普通高校先进量子点显示与照明重点实验室, 粤港澳光热能材料与器件联合实验室, 深圳市先进量子点显示与照明重点实验室, 广东 深圳 518055;<sup>3</sup>香港科技大学先进显示与光电子技术国家重点实验室, 香港 999077;<sup>4</sup>上海微系统与信息技术研究所, 上海 200050;<sup>5</sup>上海微技术工业研究院, 上海 201800

**摘要** 提出并设计了一种基于无机硒化镉(CdSe)量子点(QD)材料作为增益介质的垂直腔面发射激光器(VCSEL)。该方案结合量子点发光二极管(QLEDs)与分布式反馈布拉格反射镜(DBR)形成电注入量子点垂直腔面发射激光器,并在其垂直衬底方向上结合了电流注入结构及光学微腔结构。通过数值模拟的方法,进行了DBR反射镜参数设计、器件腔长调整等,得到了优化的器件结构。时域有限差分法模拟结果表明,设计的两种腔长器件均可实现单纵模激光,微腔品质因子超过250000。本研究提出了一种实现量子点激光二极管的新方案,并通过理论模拟进行验证,展示了此方案的可行性;同时,本工作也为下一步的实验研究提供了理论分析模型及参数指导。

**关键词** 激光器;量子点;垂直腔面发射激光器;硒化镉;时域有限差分法

中图分类号 O436

文献标志码 A

doi: 10.3788/CJL202148.1901005

## 1 引言

胶体量子点(QD)材料作为零维纳米材料,又可称为纳米晶材料,通常指材料颗粒的三维尺度都达到纳米量级,并出现明显的量子限域效应的材料<sup>[1]</sup>。由于量子限域效应,胶体量子点材料的带隙与材料颗粒尺寸密切相关并可通过化学合成的方法主动调节,进而调节量子点材料的光发射及吸收性能<sup>[1-2]</sup>。此外,量子点材料还具有窄半峰宽发射、高稳定性、发射峰温度偏移小及可溶液法加工等优势<sup>[3]</sup>,因而被广泛应用于包括发光二极管、太阳能电池、光电探测器在内的一系列光电器件中<sup>[2-4]</sup>。在量子点材料的自发辐射应用研究不断推进的同时,基于受激辐射机理的放大自发辐射及激光现象正获得越来越多

的关注。由于量子点材料的光电转换优势及可溶液法加工的特点,胶体量子点激光器有望在保持高性能高可靠性的同时极大地降低激光器的成本,具有广阔的前景及重大的现实意义。

自从首次在胶体量子点材料中实现光学增益以来<sup>[5-6]</sup>,量子点激光器领域实现了诸多重大突破,包括低温光泵浦激光器的实现、室温连续波光泵浦激光器<sup>[7]</sup>的实现以及电注入条件下实现的正光学增益<sup>[8]</sup>;目前正朝着电泵浦量子点激光二极管的目标前进<sup>[9]</sup>。通过限制光场增强耦合,多种光学谐振腔已证实可与量子点材料结合实现激光发射,如法布里-珀罗腔、分布式反馈激光腔、光子晶体微腔、回音壁模式腔、分布式布拉格微腔等<sup>[10-16]</sup>。其中,利用两面分布式布拉格反射镜的垂直腔面发射激光器结

收稿日期: 2021-06-21; 修回日期: 2021-07-29; 录用日期: 2021-08-24

基金项目: 国家科技部重大专项(2016YFB0401702, 2017YFE0120400)、国家自然科学基金(616740774, 61875082, 61405089, 62005115)、广东省重点研发计划项目(2019B010925001, 2019B010924001)、广东省大学先进量子点显示与照明重点实验室(2017KSYS007)、深圳市先进量子点显示与照明重点实验室(ZDSYS201707281632549)、深圳市孔雀团队项目(KQTD2016030111203005)

通信作者: \*sunxw@sustech.edu.cn

构具有垂直衬底发射、可晶圆级加工封装、可大批量低成本制备的优势,目前已被广泛应用在短距离光通信数据中心、激光雷达及面部识别等具体场景。基于胶体量子点材料的垂直腔面发射激光器已经实现光泵浦激射,并展现出较高品质因子带来的低阈值、可兼容柔性衬底等特性<sup>[17]</sup>。然而,已有工作在垂直腔面激光器的参数设计及性能分析方面仍有欠缺,大多采用两片分布式反馈布拉格反射镜(DBR)直接贴合的方式形成微腔;同时,电注入结构的探讨仍然有待解决<sup>[9,18-22]</sup>。

胶体量子点发光二极管已经取得长足进展,多项关键指标已经达到产业应用标准,成为下一代新型显示技术的潜在方案。在量子点发光二极管(QLEDs)器件的研究中,包括电流注入、载流子复合发光等一系列电光转换的关键问题已经得到深入探究,器件结构趋于成熟。因此,本研究提出基于 QLED 器件的胶体量子点垂直腔面发射激光器,结合 QLED 器件的电致发光功能与双面 DBR 形成光学微腔,以实现可以电光泵浦的胶体量子点垂直腔面发射激光器。主要工作集中在 DBR 设计、微腔设计、谐振波长调节等问题;通过仿真计算方法确定了器件垂直方向参数信息,实现了高品质因子的光学谐振腔设计;不仅展示了胶体量子点垂直腔面发射激光器的潜在性能优势,同时也为进一步的实验探究提供了理论分析模型和参数优化方向。

## 2 器件设计

### 2.1 垂直结构设计

如图 1 所示,本工作设计的基于胶体量子点材料的垂直腔面发射激光器主要由底层 DBR、量子点电致发光结构、顶层 DBR 构成。其中,DBR 由不同

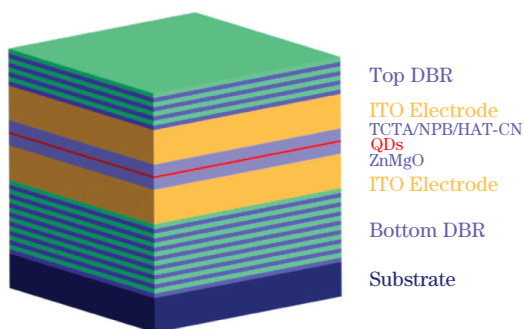


图 1 基于胶体量子点材料的垂直腔面发射激光器垂直结构示意图

Fig. 1 Schematic diagram of the designed colloidal QDs VCSEL device

折射率的介质材料交替沉积而成,并对量子点发光波段产生大于 99.9% 的反射率;上下两层 DBR 形成垂直微腔并使特定的纵模稳定谐振,产生光的限制及反馈。泵浦强度大于阈值条件后,可形成激射。提供电流注入结构的 QLED 器件为双面 ITO 电极的全透明器件,在实现电注入的同时减少了器件对于光学谐振的潜在影响;透明器件被双层 DBR 包夹在中间形成了腔内空间;同时可以通过调节氧化铟锡(ITO)透明电极的厚度来调控腔长,进而调整纵模位置,以实现有效耦合。

QLED 器件结构由 ITO/ ZnMgO/ QDs/ Tris(4-carbazoyl-9-ylphenyl)amine (TCTA)/ N,N'-di(1-naphthyl)-N,N'-diphenyl-(1,1'-biphenyl)-4,4'-diamine (NPB)/ Dipyrzino [2, 3-f; 2', 3'-h] quinoxaline-2, 3, 6, 7, 10, 11-hexacarbonitrile (HAT-CN)/ ITO 构成倒置器件,其能级结构如图 2 所示。其中,ZnMgO(30 nm)及 QDs(30 nm)基于旋涂方式制备薄膜;之后器件被转移至真空热蒸镀机进行 TCTA(10 nm),NPB(20 nm),HAT-CN(20 nm)的沉积。器件 ITO 电极由磁控溅射进行沉积,并用来控制腔长。

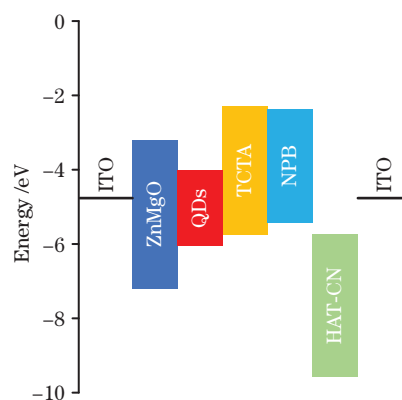


图 2 电致发光结构能级匹配示意图

Fig. 2 Schematic diagram of the energy level of the current injection structure

### 2.2 介质反射镜设计

DBR 是由两种折射率不同的材料交替生长而组成的周期性结构;当满足每层材料的光学厚度为设计的中心反射波长的  $1/4$  时,光线在每一层界面处的反射会形成相长干涉,多个周期累加后便形成高反射率。DBR 的反射谱可由传输矩阵方法进行数值计算,其反射率峰值及阻带宽度由两层介质材料的折射率差及 DBR 周期数共同决定,其中阻带宽度主要由折射率差决定,当周期数不断增加时反射率趋向饱和值。

本工作设计使用  $\text{SiN}_x/\text{SiO}_2$  和  $\text{TiO}_2/\text{SiO}_2$  两种材料组构建 DBR 反射镜,沉积工艺可根据实际使用的衬底材料进行选择。其中  $\text{SiN}_x/\text{SiO}_2$  材料可兼容标准硅基 CMOS 工艺,由等离子体增强化学气相沉积 (PECVD) 法进行沉积;而  $\text{TiO}_2/\text{SiO}_2$  材料可由磁控溅射 (sputtering) 等工艺沉积在玻璃片、硅片、石英片或柔性衬底上。

VCSEL 器件由于其腔长较短、光限制因子较小,通常需要 DBR 镜面提供大于 99.9% 的反射率才能实现对光的限制,形成谐振。图 3 计算了两种材料体系的 DBR 在周期数  $N=5, 10, 15, 20$  时的反射率谱。其中 DBR 中心波长设计为红光量子点材料典型发光峰对应的波长 630 nm;通过椭偏仪实测了几种材料在 630 nm 处的折射率  $n$  值: $n_{\text{SiO}_2}=1.44, n_{\text{TiO}_2}=2.09, n_{\text{SiN}_x}=2.04$ 。由计算结果可得:周期数  $N=5, 10, 15, 20$  的  $\text{SiN}_x/\text{SiO}_2$  DBR 在 630 nm 处的反射率分

别为 95.66831%, 99.86409%, 99.99582%, 99.99987%;周期数  $N=5, 10, 15, 20$  的  $\text{TiO}_2/\text{SiO}_2$  DBR 在 630 nm 处反射率分别为 96.74265%, 99.9202%, 99.99808%, 99.99995%。从峰值反射率数值可以发现,15 周期的介质 DBR 已经可以实现大于 99.9% 的反射率,考虑到实际制备 DBR 的成本,本研究底层 DBR 选用 15 周期结构。由于本设计中器件向上出光,顶层 DBR 选用 10 周期结构。后续计算选用  $\text{TiO}_2/\text{SiO}_2$  材料 DBR 作为基准。

### 2.3 VCSEL 腔长设计

VCSEL 器件由两面 DBR 形成谐振腔,当 DBR 确定后,腔长会显著影响器件的纵模分布。通常腔长  $L = m\lambda/(2n)$  确定,其中  $L$  为实际腔长、 $m$  为正整数、 $n$  为腔内等效折射率。由于腔内等效折射率约为 1.8,设计了  $\lambda/2, 3\lambda/2$  两种腔长,其腔长约为 175 nm 及 525 nm,如图 4 所示。

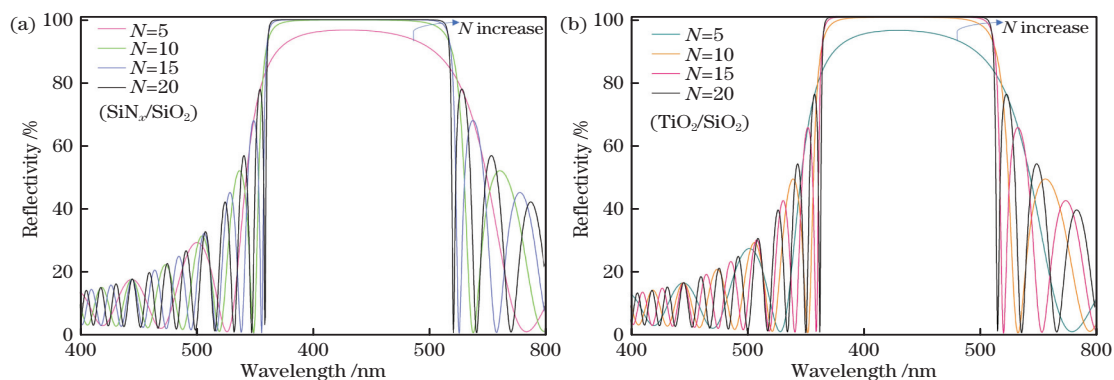


图 3 DBR 反射率谱。(a)  $\text{SiN}_x/\text{SiO}_2$  材料;(b)  $\text{TiO}_2/\text{SiO}_2$  材料

Fig. 3 Calculated reflectivity spectra of the  $\text{SiN}_x/\text{SiO}_2$  DBR and  $\text{TiO}_2/\text{SiO}_2$  DBR. (a)  $\text{SiN}_x/\text{SiO}_2$  DBR; (b)  $\text{TiO}_2/\text{SiO}_2$  DBR

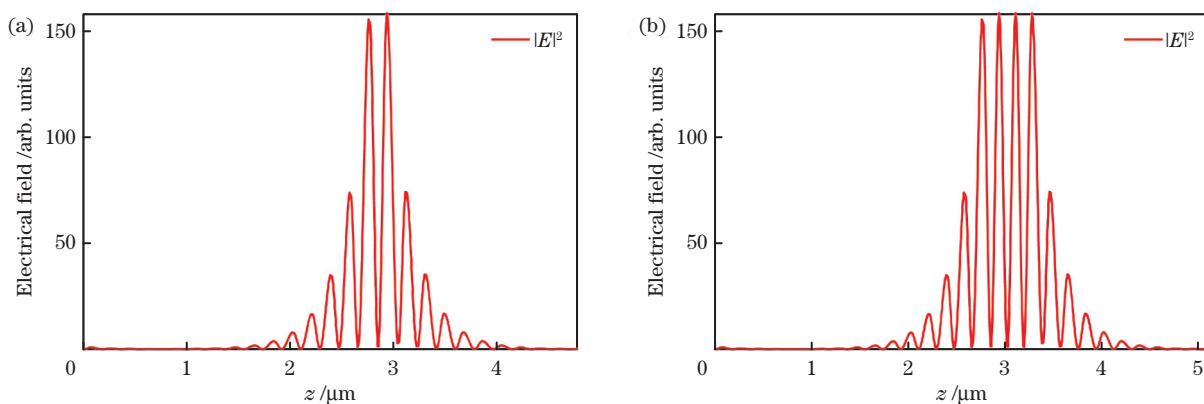


图 4 不同腔长下的驻波分布。(a)  $\lambda/2$ ;(b)  $3\lambda/2$

Fig. 4 Standing wave profile at different cavity lengths. (a)  $\lambda/2$ ; (b)  $3\lambda/2$

## 3 分析与讨论

### 3.1 $\lambda/2$ 腔长器件

在腔内电致发光结构厚度固定后,调节 ITO 厚度以控制腔长。使用时域有限差分法 (FDTD) 仿真

计算了不同 ITO 电极厚度条件下形成稳定谐振的纵模波长,并与 DBR 中心波长及量子点材料发光中心波长进行对比,以优化条件。通过 FDTD 计算发现,当上下两层 ITO 厚度为 31 nm 时,器件可实现 629.73 nm 单纵模激射,此时器件参数为优化的  $\lambda/2$

腔长。其折射率及场分布如图 5 所示。

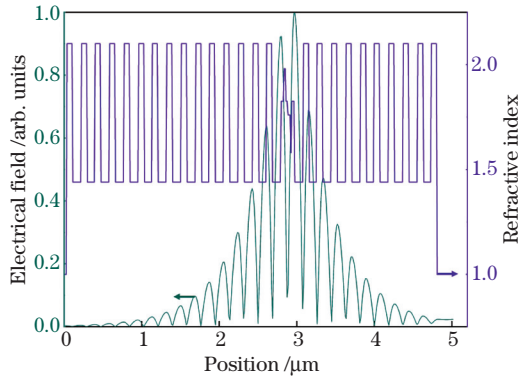


图 5 具有  $\lambda/2$  腔长的 QD-VCSEL 的折射率及光场分布  
Fig. 5 Refractive index and field distribution in  $\lambda/2$  QD-VCSEL

由于  $\lambda/2$  是理论上允许的最小腔长,故拥有最大的光限制因子。经过 FDTD 模拟,优化后的实际腔长为 172 nm,在光泵浦条件下计算得到了波长为 629.5 nm 的单纵模激射,其品质因子  $Q$  为 259632,如图 6 所示。品质因子是谐振腔的关键指标,描述了谐振腔对于震荡能量的限制能力,其定义为

$$Q = 2\pi \frac{E_2}{E_1}, \quad (1)$$

式中,  $Q$  为品质因子,  $E_2$  为谐振腔中存储的能量,  $E_1$  为每个震荡周期消耗的能量。从定义可以看出:  $Q$  值越大,表示谐振腔损耗越小;  $Q$  值越小则表示谐振腔损耗较大。

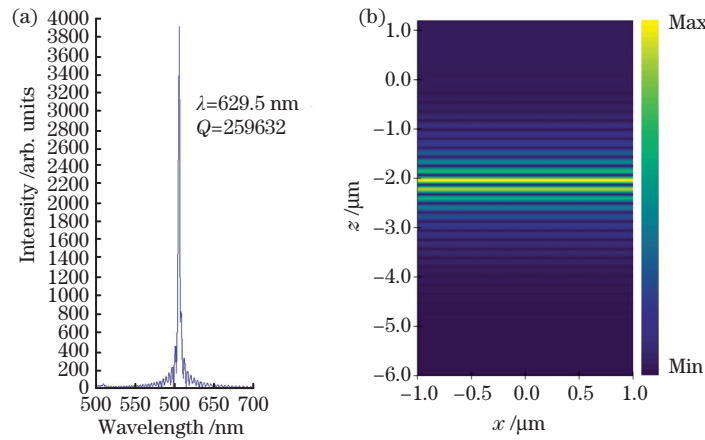


图 6  $\lambda/2$  腔长的 QD-VCSEL 的输出光谱和电场分布。(a) 输出光谱; (b) 电场分布  
Fig. 6 Output spectrum and electrical field distribution of  $\lambda/2$  QD-VCSEL.  
(a) Output spectrum; (b) electrical field distribution

### 3.2 $3\lambda/2$ 腔长器件

通过增加 ITO 电极的厚度来增大腔长,可以使腔内电注入结构保持不变。实验发现,当上下两层 ITO 厚度为 205 nm 时,器件可实现 632 nm 单纵模激射,此时器件参数为优化的  $3\lambda/2$  腔长。其折射率及场分布如图 7 所示。

由于腔长增大导致光限制因子降低,故谐振腔对光的限制有所减弱。计算优化后的实际腔长为 520 nm,在光泵浦条件下实现了波长为 632 nm 的单纵模激射,其品质因子  $Q$  为 148291,如图 8 所示。

从模式分布图中可以看出,相比短腔长器件,拥有更长腔长的器件的模式分布更为分散,不利于光场及光子的限制,因而体现出较低的品质因子。在实际实验中,更低品质因子则意味着更高的泵浦阈值功率,而这往往对器件有害。因此,即便在不同腔长的条件下都满足谐振要求,在下一步的实验验证工作中我们还是倾向于制备更短腔长的量子点垂

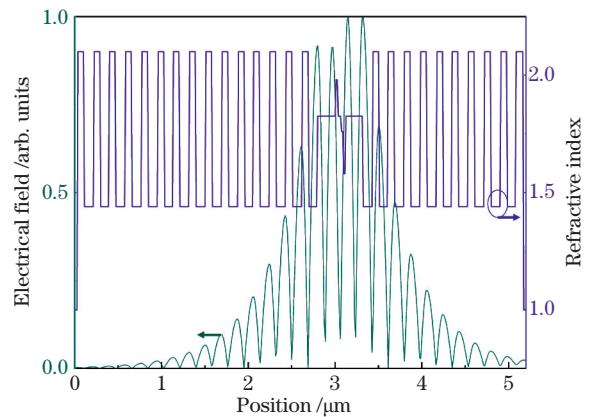


图 7 具有  $3\lambda/2$  腔长的 QD-VCSEL 的折射率及光场分布  
Fig. 7 Refractive index and field distribution in  $3\lambda/2$  QD-VCSEL

直腔面发射激光器,以实现激光出射。

图 9 展示了两种器件的一维远场分布模拟结果。在模拟过程中,通过平行于器件表面且放置在远场的一维探测器,记录器件被激发时在谐振波长

下的电场强度,从归一化的强度图可以看出,被验证器件的主要发光强度分布小于  $20^\circ$ ,在较大出射角

度的发光强度很低,光束发散情况与常规 VCSEL 相当<sup>[23-24]</sup>。

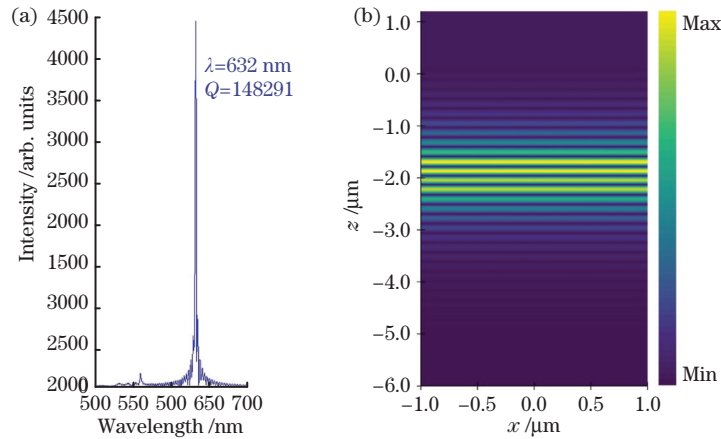


图 8  $3\lambda/2$  腔长的 QD-VCSEL 的输出光谱和电场分布。(a)输出光谱;(b)电场分布

Fig. 8 Output spectrum and electrical field distribution of  $3\lambda/2$  QD-VCSEL.

(a) Output spectrum; (b) electrical field distribution

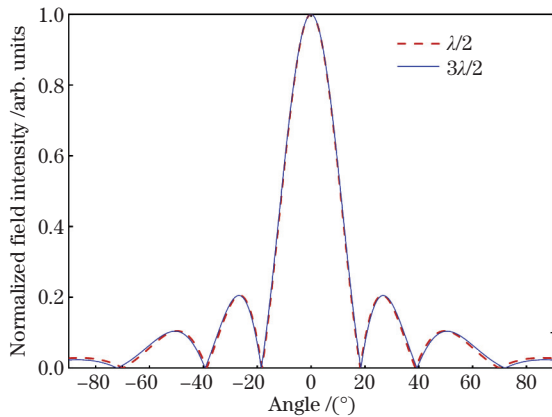


图 9 器件发光一维远场分布模拟结果

Fig. 9 Far field distribution of the simulated devices

## 4 结 论

提出了结合电致发光结构及微腔结构的量子点垂直腔面发射激光器,通过设计 DBR 和电注入结构,进行腔长调节及泵浦实验,获得了垂直腔器件的关键参数。 $\lambda/2$  腔长的 QD-VCSEL 可实现单纵模激光,同时  $Q$  值高达 259632。此工作提出了实现量子点激光二极管的新方案,为未来的实验验证提供了理论依据及参数参考。

## 参 考 文 献

[1] Kovalenko M V, Manna L, Cabot A, et al. Prospects of nanoscience with nanocrystals[J]. ACS Nano, 2015, 9(2): 1012-1057.  
 [2] Kagan C R, Lifshitz E, Sargent E H, et al. Building devices from colloidal quantum dots [J]. Science,

2016, 353(6302): aac5523.

- [3] Pietryga J M, Park Y S, Lim J, et al. Spectroscopic and device aspects of nanocrystal quantum dots[J]. Chemical Reviews, 2016, 116(18): 10513-10622.  
 [4] Kim T, Kim K H, Kim S, et al. Efficient and stable blue quantum dot light-emitting diode[J]. Nature, 2020, 586(7829): 385-389.  
 [5] Klimov V I, Mikhailovsky A A, Xu S, et al. Optical gain and stimulated emission in nanocrystal quantum dots[J]. Science, 2000, 290(5490): 314-317.  
 [6] Klimov V I, Mikhailovsky A A, McBranch D W, et al. Quantization of multiparticle auger rates in semiconductor quantum dots[J]. Science, 2000, 287(5455): 1011-1013.  
 [7] Fan F J, Voznyy O, Sabatini R P, et al. Continuous-wave lasing in colloidal quantum dot solids enabled by facet-selective epitaxy [J]. Nature, 2017, 544(7648): 75-79.  
 [8] Lim J, Park Y S, Klimov V I. Optical gain in colloidal quantum dots achieved with direct-current electrical pumping[J]. Nature Materials, 2018, 17(1): 42-49.  
 [9] Roh J, Park Y S, Lim J, et al. Optically pumped colloidal-quantum-dot lasing in LED-like devices with an integrated optical cavity[J]. Nature Communications, 2020, 11(1): 271.  
 [10] Chen Y J, Guilhabert B, Herrnsdorf J, et al. Flexible distributed-feedback colloidal quantum dot laser[J]. Applied Physics Letters, 2011, 99(24): 241103.  
 [11] Park Y S, Roh J, Diroll B T, et al. Colloidal quantum dot lasers[J]. Nature Reviews Materials, 2021, 6(5): 382-401.

- [12] Zhu Y P, Xie W Q, Bisschop S, et al. On-chip single-mode distributed feedback colloidal quantum dot laser under nanosecond pumping [J]. ACS Photonics, 2017, 4(10): 2446-2452.
- [13] Hoogland S, Sukhovatkin V, Howard I, et al. A solution-processed 1.53  $\mu\text{m}$  quantum dot laser with temperature-invariant emission wavelength [J]. Optics Express, 2006, 14(8): 3273-3281.
- [14] le Feber B, Prins F, De Leo E, et al. Colloidal-quantum-dot ring lasers with active color control[J]. Nano Letters, 2018, 18(2): 1028-1034.
- [15] Gupta S, Waks E. Spontaneous emission enhancement and saturable absorption of colloidal quantum dots coupled to photonic crystal cavity[J]. Optics Express, 2013, 21(24): 29612-29619.
- [16] Chang H, Min K, Lee M, et al. Colloidal quantum dot lasers built on a passive two-dimensional photonic crystal backbone[J]. Nanoscale, 2016, 8(12): 6571-6576.
- [17] Xie W Q, Zhu Y P, Bisschop S, et al. Colloidal quantum dots enabling coherent light sources for integrated silicon-nitride photonics[J]. IEEE Journal of Selected Topics in Quantum Electronics, 2017, 23(5): 1-13.
- [18] Grim J Q, Manna L, Moreels I. A sustainable future for photonic colloidal nanocrystals [J]. Chemical Society Reviews, 2015, 44(16): 5897-5914.
- [19] Lee Y J, Yeh T W, Zou C, et al. Graphene quantum dot vertical cavity surface-emitting lasers [J]. ACS Photonics, 2019, 6(11): 2894-2901.
- [20] Dang C, Nurmikko A, Breen C, et al. Optical gain and green/red vertical cavity surface emitting lasing from cdse-based colloidal nanocrystal quantum dot thin films [C] // CLEO: 2011-Laser Science to Photonic Applications, May 1-6, 2011, Baltimore, MD, USA. New York: IEEE Press, 2011: 1-2.
- [21] Chen J, Wang L X, Pan J Y, et al. Pumped stimulated vertical cavity surface emitting laser by solution-processed method [C]// 2019 3rd International Conference on Circuits, System and Simulation (ICCSS), June 13-15, 2019, Nanjing, China. New York: IEEE Press, 2019: 25-28.
- [22] Chen J, Du W N, Shi J W, et al. Perovskite quantum dot lasers[J]. InfoMat, 2020, 2(1): 170-183.
- [23] Liu A J. Progress in single-mode and directly modulated vertical-cavity surface-emitting lasers[J]. Chinese Journal of Lasers, 2020, 47(7): 0701005. 刘安金. 单模直调垂直腔面发射激光器研究进展 [J]. 中国激光, 2020, 47(7): 0701005.
- [24] Zhang Z, Ning Y Q, Zhang J W, et al. Design and fabrication of 1160-nm optically-pumped vertical-external-cavity surface-emitting laser [J]. Chinese Journal of Lasers, 2020, 47(7): 0701020. 张卓, 宁永强, 张建伟, 等. 1160 nm 光泵垂直外腔面发射激光器设计及制备 [J]. 中国激光, 2020, 47(7): 0701020.

## Design and Simulation of a Colloidal Quantum Dot Vertical-Cavity Surface-Emitting Laser

Xiang Guohong<sup>1,2,3</sup>, Jia Siqu<sup>1,2</sup>, Li Depeng<sup>1,2</sup>, Ma Jingrui<sup>1,2</sup>, Liu Pai<sup>1,2</sup>, Wang Kai<sup>1,2</sup>, Hoi-Sing Kwok<sup>3</sup>, Yu Mingbin<sup>4,5</sup>, Sun Xiaowei<sup>1,2\*</sup>

<sup>1</sup>Key Laboratory of Energy Conversion and Storage Technologies (Southern University of Science and Technology), Shenzhen, Guangdong 518055, China;

<sup>2</sup>Guangdong Provincial Key Laboratory for Advanced Quantum Dot Displays and Lighting, Guangdong-Hong Kong-Macao Joint Laboratory for Photonic-Thermal-Electrical Energy Materials and Devices, Shenzhen Key Laboratory for Advanced Quantum Dot Displays and Lighting, and Department of Electrical and Electronic Engineering, Southern University of Science and Technology, Shenzhen, Guangdong 518055, China;

<sup>3</sup>State Key Laboratory on Advanced Displays and Optoelectronics Technologies, The Hong Kong University of Science and Technology, Hong Kong 999077, China;

<sup>4</sup>Shanghai Institute of Microsystem and Information Technology, Shanghai 200050, China;

<sup>5</sup>Shanghai Industrial Technology Research Institute, Shanghai 201800, China

### Abstract

**Objective** Featuring wide bandgap tunability, high quantum efficiency, and cost-efficient solution processible fabrication methods, colloidal quantum dots (QDs) have been studied and applied in various optoelectronic devices including photo detectors, light-emitting diodes (LEDs), and solar cells. In addition to applications based on the

absorption and spontaneous emission of colloidal QDs, their stimulated emission potential has attracted extensive research interests, aiming toward a landmark target: the realization of the colloidal QD laser diodes. In the study of colloidal QD lasers, different laser architectures have been demonstrated, including Fabry-Perot cavity, distributed feedback laser cavity, whispering gallery mode cavity, and photonic crystal microcavity. The optical gain has been successfully realized in colloidal QDs under direct current pumping, demonstrating a major progress toward electrically pumped colloidal QD lasers. Furthermore, a dual function device based on specially engineered QDs that can function as an optically pumped laser and an LED is fabricated and characterized, revealing a promising pathway for realizing colloidal QD laser diodes. Different from edge-emitting lasers, vertical-cavity surface-emitting lasers exhibiting surface-emitting properties, wafer-level fabrication & characterization capability, and array integration ability have been widely used in optical fiber communication, laser printers, computer mouse, and three-dimensional facial recognition fields, etc. Here, we propose and design a colloidal quantum dots vertical cavity surface emitting laser, combining with a quantum dots light-emitting diode like current injection structure to realize the electroluminescence ability.

**Methods** As shown in Fig. 1, the QLED-like structure containing the QD gain medium is sandwiched by two high-reflective distributed feedback reflectors to form a vertical-cavity surface-emitting laser (VCSEL)-like device. The device is designed to work under optical or electrical pumping. The DBR parameters and cavity lengths, are determined by numerical simulations with optimal performance. A DBR mirror is formed by periodically arranging two materials with different refractive indices. The reflectance spectrum is determined by both the DBR materials and DBR periods. Herein, we designed and calculated two types of DBRs with different periods (Fig. 3): (a)  $\text{SiN}_x/\text{SiO}_2$  DBR and (b)  $\text{TiO}_2/\text{SiO}_2$  DBR. It is found that 10 periods of the designed dielectric DBR can realize a peak reflectance of greater than 99%. The cavity length is a crucial parameter of the VCSEL device. After determining the DBR parameters, the permitted longitude modes inside the cavity can be tuned using the cavity length. Here, we use the FDTD method to build the designed QD-VCSEL device model and sweep the cavity length parameter. The current injection structure along the vertical direction includes the QD gain materials, electron and hole transmission layers, and electrodes. To tune the effective cavity length while retaining the optimized current injection capability, transparent ITO electrodes are selected and designed according to a suitable thickness. By theory, the smallest cavity length of a VCSEL device is  $\lambda/2$ . Thus, based on this length, the current injection structure and the thickness of the gain medium are fixed, while the thickness of the transparent ITO electrode is used to change the cavity length and then tune the resonant mode (Fig. 5). In addition to the  $\lambda/2$  cavity length device, a  $3\lambda/2$  cavity length device is designed and simulated to theoretically optimize the optical parameters.

**Results and Discussions** Under optical excitation, the designed  $\lambda/2$  cavity length QD-VCSEL device can support single-mode lasing at 629.5 nm with a cavity length of 172 nm. The calculated quality factor is 259632. Alternatively, the  $3\lambda/2$  cavity length device can be optimized with a 520-nm cavity length. The lasing mode is realized at 632 nm, and the quality factor is 148291. Compared to the cavity with the smallest cavity length, a longer cavity suffers further optical loss while facilitating a thicker gain region. However, a considerably longer cavity length is not favored because of the difficulty in the formation of a very thick QD layer with a high concentration. The simulated far-field pattern reveals that the designed devices achieve a low output beam divergence, comparable to conventional VCSEL devices, which is an intrinsic advantage of this type of semiconductor laser. This work proposes a new scheme for realizing QD laser diodes, providing a theoretical basis and a parameter reference for future experimental verification.

**Conclusions** In this work, a CdSe QD vertical-cavity surface-emitting laser is designed. The QD-VCSEL device is simulated with a QLED-like structure sandwiched by two dielectric DBR mirrors. The DBR parameters and cavity lengths are determined by numerical simulations with optimal performance. Single-longitude mode lasing can be supported by two designed cavities with different lengths with a maximum quality factor  $Q$  over 250000. The new solution toward electrically pumped colloidal QD lasers is revealed with our design, along with the theoretical model and key factors, which can be helpful in subsequent experimental work.

**Key words** lasers; quantum dots; vertical cavity surface emitting laser; CdSe; finite difference time domain method

**OCIS codes** 250.5590; 250.7260; 250.7270; 260.5740